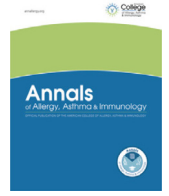




Since January 2020 Elsevier has created a COVID-19 resource centre with free information in English and Mandarin on the novel coronavirus COVID-19. The COVID-19 resource centre is hosted on Elsevier Connect, the company's public news and information website.

Elsevier hereby grants permission to make all its COVID-19-related research that is available on the COVID-19 resource centre - including this research content - immediately available in PubMed Central and other publicly funded repositories, such as the WHO COVID database with rights for unrestricted research re-use and analyses in any form or by any means with acknowledgement of the original source. These permissions are granted for free by Elsevier for as long as the COVID-19 resource centre remains active.



# Patients with coronavirus disease 2019 characterized by dysregulated levels of membrane and soluble cluster of differentiation 48



Hadas Pahima, PhD<sup>\*</sup>; Ilan Zaffran, MSc<sup>\*</sup>; Eli Ben-Chetrit, MD<sup>†</sup>; Amir Jarjoui, MD<sup>†</sup>; Pratibha Gaur, PhD<sup>\*</sup>; Maria Laura Manca, PhD<sup>‡</sup>; Dana Reichmann, PhD<sup>§</sup>; Efrat Orenbuch-Harroch, MD<sup>||</sup>; Ekaterini Tiligada, PhD<sup>\*,¶</sup>; Ilaria Puxeddu, MD, PhD<sup>#</sup>; Carl Zinner, MD<sup>\*\*</sup>; Alexandar Tzankov, MD, PhD<sup>\*\*</sup>; Francesca Levi-Schaffer, PharmD, PhD<sup>\*</sup>

<sup>\*</sup> Pharmacology and Experimental Therapeutics Unit, School of Pharmacy, Institute for Drug Research, Faculty of Medicine, The Hebrew University of Jerusalem, Jerusalem, Israel

<sup>†</sup> Infectious Diseases Unit, Faculty of Medicine, Department of Medicine, Shaare Zedek Medical Center, Hebrew University of Jerusalem, Israel

<sup>‡</sup> Department of Clinical and Experimental Medicine, University of Pisa, Pisa, Italy

<sup>§</sup> Department of Biological Chemistry, The Alexander Silberman Institute of Life Sciences, Safra Campus Givat Ram, The Hebrew University of Jerusalem, Jerusalem, Israel

<sup>||</sup> Medical Intensive Care Unit, Hadassah-Hebrew University Medical Center, Ein Kerem Campus, Jerusalem, Israel

<sup>¶</sup> Department of Pharmacology, Medical School, National and Kapodistrian University of Athens, Athens, Greece

<sup>#</sup> Immunology and Allergology Unit, Department of Clinical and Experimental Medicine, University of Pisa, Pisa, Italy

<sup>\*\*</sup> Institute of Pathology, University Hospital Basel, Schönbeinstrasse, Basel, Switzerland

## ARTICLE INFO

### Article history:

Received for publication August 2, 2022.

Received in revised form October 13, 2022.

Accepted for publication October 13, 2022.

## ABSTRACT

**Background:** Coronavirus disease 2019 (COVID-19), caused by the severe acute respiratory syndrome coronavirus 2 (SARS-CoV-2), can progress into a severe form of acute lung injury. The cosignaling receptor cluster of differentiation 48 (CD48) exists in membrane-bound (mCD48) and soluble (sCD48) forms and has been reported to be implicated in antiviral immunity and dysregulated in several inflammatory conditions. Therefore, CD48 dysregulation may be a putative feature in COVID-19-associated inflammation that deserves consideration.

**Objective:** To analyze CD48 expression in lung autopsies and peripheral blood leukocytes and sera of patients with COVID-19. The expression of the CD48 ligand 2B4 on the membrane of peripheral blood leukocytes was also assessed.

**Methods:** Twenty-eight lung tissue samples obtained from COVID-19 autopsies were assessed for CD48 expression using gene expression profiling immunohistochemistry (HTG autoimmune panel). Peripheral whole blood was collected from 111 patients with COVID-19, and the expression of mCD48 and of membrane-bound 2B4 was analyzed by flow cytometry. Serum levels of sCD48 were assessed by enzyme-linked immunosorbent assay.

**Results:** Lung tissue of patients with COVID-19 showed increased CD48 messenger RNA expression and infiltration of CD48+ lymphocytes. In the peripheral blood, mCD48 was considerably increased on all evaluated cell types. In addition, sCD48 levels were significantly higher in patients with COVID-19, independently of disease severity.

**Conclusion:** Considering the changes of mCD48 and sCD48, a role for CD48 in COVID-19 can be assumed and needs to be further investigated.

© 2022 American College of Allergy, Asthma & Immunology. Published by Elsevier Inc. All rights reserved.

Dr Pahima and Mr Zaffran contributed equally to this article, and both should be considered first author.

**Reprints:** Francesca Levi-Schaffer, PharmD, PhD, Isaac & Myrna Kaye Chair in Immunopharmacology, Pharmacology & Experimental Therapeutics Unit, Institute for Drug Research, School of Pharmacy, Faculty of Medicine, The Hebrew University of Jerusalem, Jerusalem, Israel. E-mail: francescal@ekmd.huji.ac.il.

**Disclosures:** The authors have no conflicts of interest to report.

**Funding:** This work was supported by grants from the Israel Science Foundation (ISF, 3933/19) to Dr Levi-Schaffer and the Israeli Scholarship Education Foundation to Mr Zaffran. Dr Tiligada was awarded a Lady Davies Fellowship as visiting professor in Dr Levi-Schaffer's laboratory.

## Introduction

Cluster of differentiation (CD) 48 (also referred to as signaling lymphocytic activation molecule family 2) is a glycosyl-phosphatidylinositol-activating or coactivating receptor expressed on most hematopoietic cells, similarly to its high-affinity ligand 2B4 (CD244), which is also a member of the signaling lymphocytic activation molecule family of receptors that has been implicated in antiviral immunity. Similarly to several other glycosyl-phosphatidylinositols, CD48 exists in both membrane-bound (mCD48) and soluble (sCD48) forms.<sup>1</sup> Interestingly, sCD48 levels are elevated in the sera of patients

infected with the Epstein-Barr virus<sup>2</sup> or with the varicella-zoster virus.<sup>3</sup> In addition, measles infections are accompanied by increased expression of mCD48 on monocytes and lymphocytes.<sup>3</sup> Moreover, the owl monkey cytomegalovirus (CMV) has been reported to use the decoy property of sCD48 and to produce sCD48 homologues to escape the immune response.<sup>4</sup>

Coronavirus disease 2019 (COVID-19) is a respiratory-centered systemic disorder caused by the severe acute respiratory syndrome coronavirus 2 (SARS-CoV-2). The first case was described in December 2019, and by mid-September 2022, more than 600 million cases and 6.5 million deaths had been reported worldwide, according to the World Health Organization. Most individuals infected with SARS-CoV-2 are asymptomatic or experience mild symptoms.<sup>5</sup> However, the disease can progress into a severe form, causing acute lung injury (ALI), mainly diffuse alveolar damage (DAD) with thromboinflammation, immunopathology, and cytokine storm syndrome.<sup>6</sup> Interleukin (IL)-6 is one of the cytokines involved in progressive and severe disease and was suggested together with C-reactive protein (CRP) to be a useful predictor for patients requiring mechanical ventilation.<sup>7</sup>

Similarly to SARS-CoV-2, other viral pathogens play an important role in many respiratory pathologies,<sup>8,9</sup> such as asthma, in which CD48 has been identified as a putative immunoinflammatory player. Interestingly, in moderate asthma, mCD48 is increased on peripheral blood eosinophils and B cells, whereas in severe asthma, mCD48 is increased on B cells, T cells, NK cells, and monocytes. Soluble CD48 levels are significantly increased in the sera of patients with mild asthma compared with those of healthy donors, whereas patients with severe asthma treated with glucocorticosteroids display decreased levels of sCD48.<sup>10</sup> However, the decrease in sCD48 seemed to be owing to asthma severity rather than to a direct effect of the drug.<sup>11</sup> Importantly, CD48 increase in asthma was correlated neither with T<sub>H</sub>2 inflammation biomarkers such as IL-33, IL-5, immunoglobulin E, and eosinophil numbers nor with tobacco smoking or body mass index (BMI).<sup>12</sup>

On the basis of the above presented evidence, especially on the role that CD48 seems to play in asthma and viral infections, we aimed at investigating the potential dysregulation of CD48 and its ligand expression in COVID-19. We report on the findings obtained after *in situ* analysis of CD48 expression in postmortem lung specimens and examination of mCD48 expression on peripheral blood cells and of sCD48 in serum of patients with COVID-19 with various disease severities.

## Methods

### Study Cohort

Lung tissues from 28 patients who died from COVID-19 (eTable 1) during the first disease wave in Switzerland (March–May 2020) were collected and organized into a tissue microarray (TMA) format, as reported previously.<sup>13,14</sup> Moreover, 10 DAD, 5 influenza pneumonia, 13 hypertensive disease, 15 normal lung, and 9 bacterial pneumonia tissue samples were collected and used as control diseases. The original paraffin blocks of each patient specimen were punched 3 times with a 1-mm core needle. For the purposes of the study, areas of superposed pneumonia were excluded, to obtain informative samples from the areas of primary COVID-19–related damage.

Tissue collection was approved by the Ethics committee of Northern and Central Switzerland (study ID 2020-00969). No patient with COVID-19, except 1 treated with low dose prednisone, had been treated with oral corticosteroids; in particular, none had received dexamethasone as per treatment protocols established later in the pandemic. Samples were taken 11.0 to 84.5 hours (mean 33.2 hours) after death from COVID-19. The range of the time length between diagnosis of COVID-19 and death was 0 to 20 days (mean 7.15 days). The hospitalization length of time before death was 0 to 16 days

(mean 5.7 days). In all cases, the postmortem viral load was measured in lungs by a quantitative reverse transcription polymerase chain reaction (PCR) assay as reported previously.<sup>13</sup> The RNA from formalin-fixed paraffin-embedded tissue was extracted with the RecoverAll Total Nucleic Acid Isolation Kit (Thermo Fisher Scientific, Waltham, Massachusetts). Viral genomes were detected with the TaqMan 2019-nCoV Assay Kit v1 (Thermo Fisher Scientific), which targets 3 different viral genomic regions (ORF1b, S protein, and N protein) and the human RNase P gene (RPPH1). The number of viral genomes was determined with the TaqMan 2019-nCoV Control Kit v1 (Thermo Fisher Scientific) and a comparative C<sub>T</sub> ( $\Delta\Delta C_T$ ) method. The method generates individual copy numbers for human RPPH1 and the 3 SARS-CoV-2 targets. Mean copy numbers of SARS-CoV-2 targets were scaled to  $1 \times 10^6$  RPPH1 copies. The viral load was assessed by calculating the log of the median of the 3 SARS-CoV-2 protein (ORF, S, and N).

Blood was obtained from 111 patients with active COVID-19 (eTable 2 and eTable 3) and 18 patients recovered from COVID-19 (eTable 4), hospitalized either in Shaare Zedek Medical Center (86 patients; P1–P86) or Hadassah University Hospital (5 patients; P87–P91 and 2 recovered; R1–R2) (Jerusalem, Israel) and in Pisa University Hospital (20 patients; P92–P11 and 15 recovered; R3–R18) (Pisa, Italy), and from 26 age- and sex-matched healthy controls (eTable 5) in Hadassah University Hospital (Jerusalem, Israel). Patients were classified for disease severity according to World Health Organization guidelines.<sup>15</sup> The study included 26 patients with mild, 20 patients with moderate, 49 patients with severe, and 16 with critical disease. The blood collection time after swab test ranged from 1.0 to 24.0 days (mean 4.8 days) for the patients with active COVID-19 and after 2 negative PCR tests for the patients who recovered. The collection of peripheral blood and the experimental procedures were approved by the Declaration of Helsinki committee of each hospital.

### Gene Expression Programming of Lung Tissue

Gene expression programming (GEP) of the lung tissue obtained at autopsy and used for the TMA construction was performed by HTG according to established protocols<sup>16</sup> (<https://www.htgmolecular.com/assets/htg/resources/BR-05-HTG-EdgeSeq-System.pdf>). Lysates from samples were run on the HTG EdgeSeq Processor (HTG Molecular Diagnostics, Tucson, Arizona) using the HTG EdgeSeq Immune Response Panel with an excess of nuclease protection probes (NPPs) complementary to their target. S1 nuclease then removed unhybridized probes and RNAs, leaving behind nuclease protection probes hybridized to their targets in a 1:1 ratio. Samples were individually barcoded using a 16-cycle PCR to add adapters and molecular barcodes, individually purified using AMPure XP beads (Beckman Coulter, Brea, California), and quantitated using a KAPA Library Quantification kit (KAPA Biosystems, Wilmington, Massachusetts). Libraries were sequenced on the Illumina SEQUENCER platform (Illumina, San Diego, California) for quantification. Quality control, standardization, and normalization were performed by HTG and provided to the investigators. Quality control criteria as determined by the manufacturer (percentage of overall reads allocated to the positive process control probe per sample  $\leq 28\%$ , read depth  $\geq 750,000$ , relative SDs of reads of each probe within a sample  $\geq 0.094$ ) were met for all samples.

Data were first analyzed by the HTG online tool (<https://reveal.htgmolecular.com/>), including manual analysis of the genes of interest. A principal components analysis was then performed using the pcomp function in R, version 4.0.3 (R-Project for Statistical Computing, Vienna, Austria), and differential expression analysis of COVID-19 cases against controls was conducted with the DESeq2 package, using default settings. Count estimates were normalized with the median ratio method, and 6 low-quality samples were excluded from

analysis for 26 COVID-19 cases, 10 DAD, 13 hypertensive lung, 4 influenza, 15 normal, and 6 bacterial pneumonia cases. Before the heatmap visualization, the normalized counts were further transformed using a robust variance stabilization. The heatmap was produced with the pheatmap package. The column clusters of the samples and the row clusters of the significant genes were obtained by hierarchical clustering with complete linkage and a Euclidean distance metric. The Wald test statistic was used, and *P* values were adjusted for false discoveries. Adjusted *P* values  $\leq .05$  and  $|\log_2(\text{fold change})| \geq 1$  were considered significant and included in the analysis.

### Immunohistochemistry

Except for CD48 (below), immunohistochemistry (IHC) was performed on the TMAs using the automated staining system Benchmark XT (Ventana Medical Systems [Roche], Tucson, Arizona) as per ISO15189 accredited standard operating procedure of the Institute of Pathology at the University Hospital Basel. In situ hybridization for SARS-CoV-2 was performed as previously reported.<sup>17</sup> For CD48 IHC, slides from the 28 patients who died from COVID-19 were compared with similarly arrayed cases of 5 influenza viral pneumonias, 5 pneumococcal pneumonias, 9 other causes (noninfectious and non-COVID-19) DAD (referred to as “other cause DAD”), and 5 normal lung samples (control tissues), all chosen randomly (eTable 6). Slides were stained by Dako autostainer after deparaffinization by warming up to 75°C. Antigen retrieval was achieved at 95°C with the Ultra Cell Conditioner, for 8 minutes. Slides were then incubated for 40 minutes at 37°C with 6.9 µg/mL of anti-CD48 antibody (EPR4108; ab134049; Abcam, Cambridge, United Kingdom) or secondary antibody only as a negative control, washed, and counterstained with hematoxylin (Gill II).

Stained sections were scanned using the Aperio AT2 scanner (Leica, Wetzlar, Germany). Images were visualized using Aperio ScanScope Console, and 3 different lung sections (superior, middle, and inferior lobes, right and left) from each patient were analyzed manually according to the following pattern scale: “pattern one” referred to less than 10% CD48 positive lymphocytes in the alveolar septa, whereas more than 10% cells were considered as “pattern two.” “Pattern three” corresponded to the presence of subtle CD48-positive lymphocyte exudation in the intra-alveolar space and “pattern four” to the heavy intra-alveolar exudation of CD48-positive cells. The decision whether lymphocytes were stained for CD48 was based on microscopic analysis.

### Leukocyte Isolation From Peripheral Blood of Patients With Coronavirus 2019 and Controls

The white blood cell fraction from peripheral blood of patients with COVID-19 and of healthy controls was isolated according to a previously described protocol.<sup>10</sup> Granulocytes and mononuclear cells were obtained, washed, and resuspended in flow cytometry (FC) buffer containing 0.5% bovine serum albumin (BSA) and 2% fetal bovine serum in PBSX1. For serum collection, venous blood (1–2 mL) was withdrawn in nonheparinized tubes and centrifuged (2000 rpm, 10 minutes, 4°C). The collected serum was stored at –80°C.

### Human Peripheral Blood Leukocytes Double Staining

Isolated fractions of granulocytes and mononuclear cells ( $2 \times 10^5/100 \mu\text{L}$  of 0.1% BSA in phosphate buffered saline [PBS]) were incubated in 96 U-bottom plates (Thermo Fisher Scientific Inc) on ice. For FC double staining, cells were blocked (5% goat serum, 0.1% BSA in PBS 15 minutes on ice) and incubated with either fluorescein isothiocyanate (FITC)-antihuman CD3 (clone HIT3a; BioLegend, San Diego,

California) and PE-antihuman CD56 (NCAM) (HCD56; BioLegend) for T cells and NK cells, FITC-antihuman CD20 (2H7; BioLegend) for B cells, FITC-antihuman CD14 (HCD14; BioLegend) for monocytes, or FITC-antihuman CD16 (3G8; Santa Cruz Biotechnology, Dallas, Texas) for neutrophils. For the analysis of cell surface molecules, cells were stained with APC-antihuman CD48 (MEM-102; Abcam); APC-antihuman 2B4 (CD244) (2-69; BioLegend); or with the isotype control APC-mouse immunoglobulin G1 (MOPC-21; BioLegend). Thereafter, cells were washed twice (300 g, 5 minutes, 4°C) with 0.1% BSA in PBS, and FC data were acquired by BD LSR II Flow Cytometer and analyzed with FlowJo software (Tree Star, Oregon). Cell populations were gated according to physical parameters and surface marker specific staining (eFig 1). Mean fluorescence intensities were determined by dividing the fluorescence intensity of the specific mAb by that of the isotype control. eFigure 1C shows a representative histogram of mCD48 staining.

### Measurement of Soluble Cluster of Differentiation 48 and Interleukin-6 Levels in Serum

Serum levels of sCD48 and IL-6 were quantified using commercially available enzyme-linked immunosorbent assay (ELISA) kits (human CD48 ELISA kit; DEIA237 Sensitivity: 9.38 pg/mL; Creative Diagnostic, Shirley, New York; and Deluxe set Human IL-6, cat: 430504 Sensitivity: 4 pg/mL; BioLegend) according to the manufacturer's instructions. Interleukin-6 and sCD48 ELISA tests were performed in duplicates using undiluted serum and 1:40 diluted, respectively, and values were calculated on the basis of a recombinant standard curve.

### Statistical Analysis

Continuous data are expressed as mean  $\pm$  SEM, or median and interquartile range. Variables with a skewed distribution (by the Shapiro-Wilk test) were log-transformed for use in parametric testing. Statistical comparisons between experimental groups were performed using one-way analysis of variance and post hoc Tukey's multiple comparison tests. For fewer than 3 experimental groups, Student's unpaired 2-tailed *t* test was used. Associations were evaluated by Spearman correlation testing. Data were analyzed by Prism version 9.0 (GraphPad Software, San Diego, California). A *P* value less than .05 was considered statistically significant for all analyses.

## Results

### Laboratory Findings

Routine blood tests of patients with COVID-19 and healthy controls are shown in Figure 1 and Table 1. As expected, patients with COVID-19 displayed peripheral blood neutrophilia (Fig 1A), lymphocytopenia (Fig 1B), and eosinopenia (Fig 1C) and significant upregulation of CRP (Fig 1D) and IL-6 (Fig 1E) levels that were associated with disease severity. Similarly to a previous report,<sup>18</sup> patients who were critically ill and patients with severe disease showed a significant decrease in hemoglobin levels (Fig 1F) and nonsignificantly increased levels of D-dimer and ferritin levels (eFigure 2A, and B).

### Lung Tissue of Patients with Coronavirus 2019 Displays Significantly Higher Cluster of Differentiation 48 Messenger RNA Levels Than Other Lung Pathologies and Increased Infiltration of Cluster of Differentiation 48-Positive Lymphocytes Compared With Other Lung Pathologies

To assess the expression levels of CD48 in the lung tissues of patients with COVID-19, a transcriptomic analysis was performed. The messenger RNA (mRNA) levels of *CD48* were found to be significantly upregulated in COVID-19 lung tissue in comparison with those

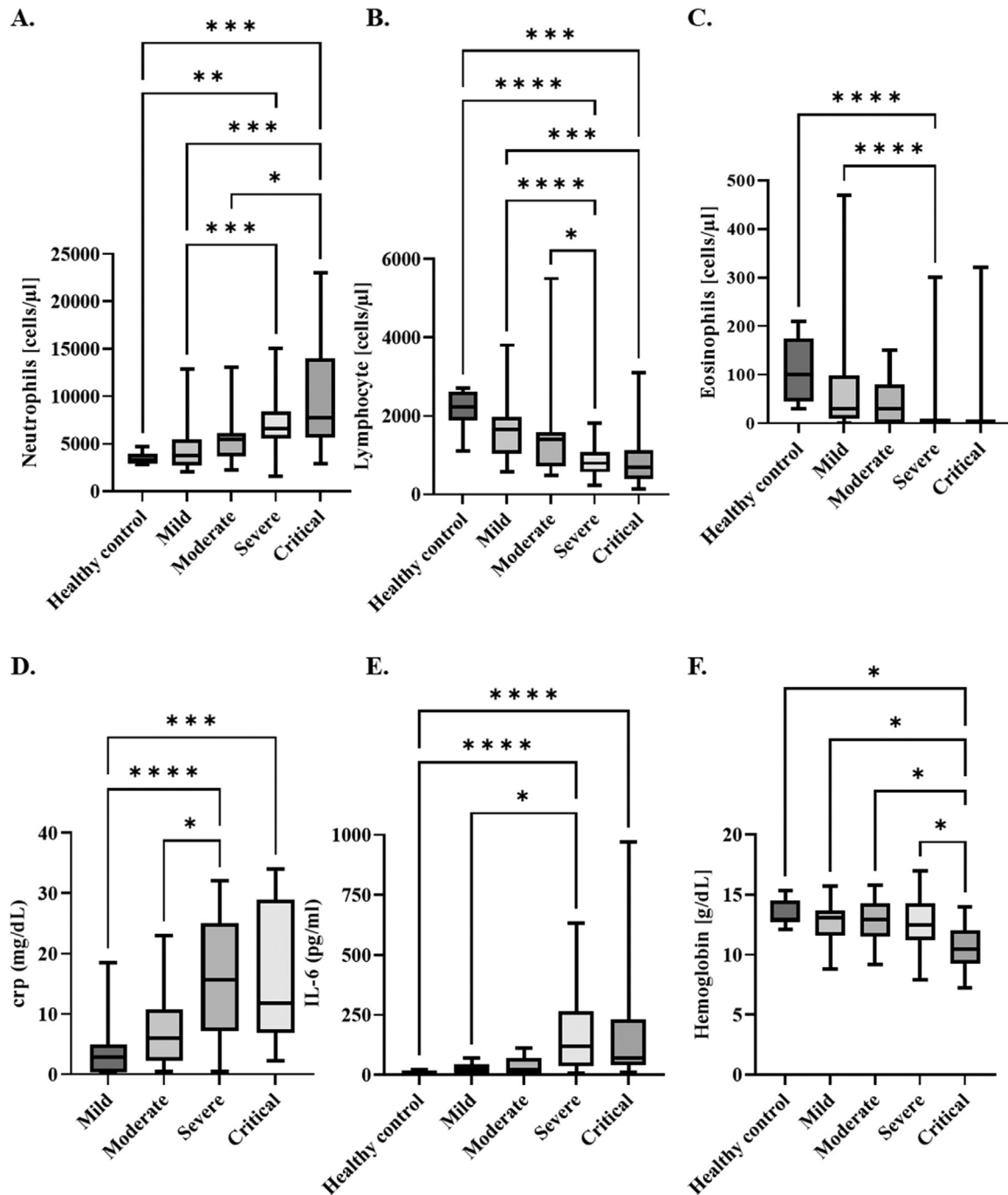


**Figure 1.** Laboratory findings in patients with COVID-19 and in healthy controls: (A) Neutrophils (cells/ $\mu$ L); (B) Lymphocytes (cells/ $\mu$ L); (C) Eosinophils (cells/ $\mu$ L); (D) CRP levels (mg/dL); (E) IL-6 (pg/mL) levels; (F) Hemoglobin (g/dL) from patients with COVID-19 and/or healthy controls. Data are shown as the mean  $\pm$  SEM. Asterisk denotes  $P < .05$ , double asterisks denote  $P < .01$ , triple asterisks denote  $P < .001$ , four asterisks denote  $P < .0001$ . COVID-19, coronavirus disease 2019; CRP, C-reactive protein.

**Table 1**  
Laboratory Findings of Patients With Active COVID-19, With Different Disease Severities

	Ferritin		D-dimer		Creatinine		CRP	
	mean	n	mean	n	mean	n	mean	n
Mild	151.2 $\pm$ 533.5	17	128.0 $\pm$ 742.3	19	0.29 $\pm$ 1.263	24	0.89 $\pm$ 4.051	25
Moderate	307.7 $\pm$ 544.8	6	350.6 $\pm$ 944.7	11	0.067 $\pm$ 0.787	16	1.47 $\pm$ 6.749	16
Severe	123.4 $\pm$ 749.2	32	1259 $\pm$ 4026	38	2.411 $\pm$ 5.910	49	1.34 $\pm$ 13.69	49
Critical	1868 $\pm$ 3220	13	3210 $\pm$ 6822	14	5.240 $\pm$ 6.974	16	2.80 $\pm$ 15.71	16

Abbreviations: COVID-19, coronavirus disease 2019; CRP, C-reactive protein.

NOTE. Data presented as mean  $\pm$  SEM.



of overall controls (false discovery rate-adjusted  $P$  value  $\leq .01$ ) (Fig 2A, and B) and especially in comparison with DAD and healthy controls (eTable 7). Moreover, mRNA levels of *CD48* were found to be associated in COVID-19 with the expression of genes related with T cells (*CD3G/E/D*, *CD8A*, *CD4*) and NK cells (*CD160*, *CD2*, *NCAM1*, *NRG7*) but not with B cells (*CD27*, *MS4A1 [encoding for CD20]*, *CD19*, *PAX5*) (Fig 2A). Messenger RNA levels of *2B4* were also found slightly increased in COVID-19 lung sections in comparison with DAD, contrary to influenza samples in which *2B4* was downregulated and therefore appeared to be increased in COVID-19 (Fig 2A). Consistent with the mRNA data, *CD48* immunostaining patterns showed a general increase of “pattern four” in COVID-19 in comparison with the other lung pathologies (Fig 2B). Importantly, *CD48* positive (*CD48* $\pm$ ) lymphocytes were the predominant infiltrating cells in COVID-19 lung tissues (Fig 2C), as confirmed by morphologic analysis. Of note, non-COVID-19 DAD lungs showed mostly “pattern three,” even though they displayed significant amounts of *CD48* negative intra-alveolar immune cell infiltration.

#### *Increased Cluster of Differentiation 48 on Circulating Leukocytes and in Serum of Patients With Coronavirus 2019*

Next, we evaluated m*CD48* expression on peripheral blood T cells, B cells, NK cells, monocytes, and neutrophils from patients with COVID-19 with different disease severity and from healthy controls. Interestingly, the expression levels of m*CD48* were significantly higher on all patient cell types studied than on their counterparts derived from healthy volunteers (Fig 3A–E, Table 2). The highest increase was found on monocytes (2.2-fold) and NK cells (2-fold). The *CD48* expression on neutrophils was almost undetectable and increased only by 1.3-fold. (Fig 3E, Table 2). Interestingly, m*CD48* expression enhancement was not linked to disease severity, except for B cells, in which m*CD48* expression was significantly increased in patients with mild-to-moderate compared with severe-to-critical disease (eFig 3A).

Moreover, s*CD48* levels were significantly higher in patients with COVID-19 than in the healthy control group (Fig 3F, Table 3). However, the observed increases were not associated with immunosuppressive treatment (eFig 3B) or disease severity because similar values were obtained for mild, moderate, severe, and critical disease (eFig 3C, Table 3). It is noteworthy that s*CD48* levels in patients who had recovered from the disease were similar to those observed in healthy controls (Fig 3F, Table 3). Interestingly, s*CD48* was negatively correlated ( $r = -0.3548$ ,  $P$  value = .002) with platelet numbers (eFig 3D). Moreover, in the serum of patients with mild COVID-19, the levels of s*CD48* were significantly correlated with either IL-6 ( $r = 0.6079$ ,  $P$  value = .047) or CRP ( $r = 0.5783$ ;  $P$  value = .008) levels (eFig 3E,F).

#### *Up-regulation of Membrane-Associated 2B4 Levels in Natural Killer Cells and Monocytes in Patients With Coronavirus 2019*

The levels of m2*B4* were evaluated on blood leukocytes from patients with COVID-19 and from healthy controls. Membrane-bound 2*B4* levels were found to be significantly elevated on NK cells (Fig 4A) and monocytes (Fig 4B) in comparison with those of healthy controls, whereas on B cells, T cells, and neutrophils, m2*B4* levels were undetectable. High levels of m2*B4* on NK cells were positively correlated with high levels of m*CD48* on either T cells ( $r = 0.8573$ ;  $P$  value = .007), monocytes ( $r = 0.7114$ ;  $P$  value = .047), or NK cells ( $r = 0.8703$ ;  $P$  value = .007) (Fig 4C–E). It is noteworthy that the correlation between m2*B4* on NK cells and m*CD48* on either monocyte ( $r = 0.6297$ ;  $P$  value = .03) or NK cells was also found in healthy controls ( $r = 0.6939$ ;  $P$  value = .01), whereas the respective correlations with T cells were detected only in the patients' cells (Fig 4F–H).

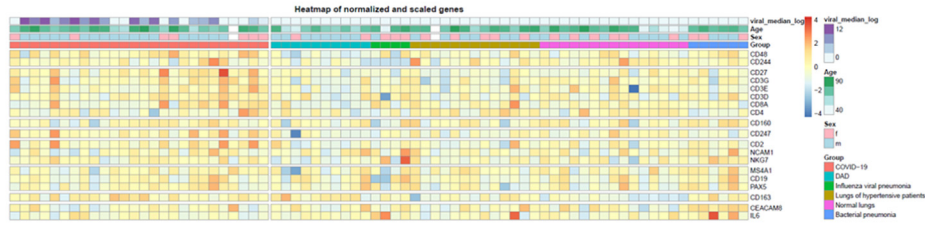
## Discussion

This study provides a comprehensive report on the effect of SARS-CoV-2 infection on the expression of *CD48* in the lungs and in the peripheral blood of patients with COVID-19. To investigate the influence of SARS-CoV-2 infection on lung *CD48* expression, we examined postmortem lung tissue obtained from patients with COVID-19, from individuals with other lung pathologies such as non-COVID-19 DAD, influenza pneumonia, and pneumococcal pneumonia, and from individuals with normal lungs.

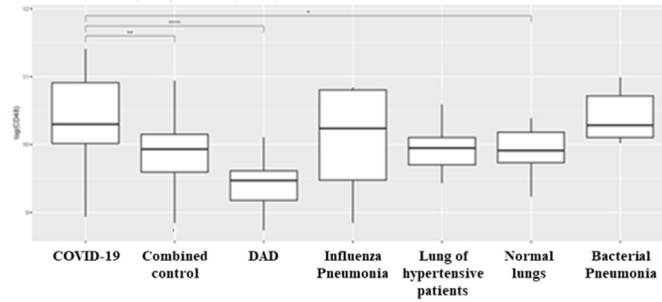
The acute lung injury caused by SARS-CoV-2 infection was reported to have many morphologic similarities to non-COVID-19 DAD.<sup>6</sup> However, some COVID-19-related characteristics have been observed, including massive capillarostasis, intussusceptive angiogenesis, and a massive increased neutrophil extracellular trap-related cell death called NETosis.<sup>6</sup> Here, we report that the significant upregulation of *CD48* mRNA in the affected lungs is an additional COVID-19-related parameter in DAD. This finding suggests that *CD48* levels may increase either because of SARS-CoV-2 infection or because of the lung injury caused by the virus. This is an important additional observation to differentiate between DAD induced by SARS-CoV-2 and DAD induced by toxic and other infectious agents. Notably, the augmented mRNA levels of *CD48* were associated with increased mRNA levels of *CD8*-expressing (*CD8* $\pm$ ) T-cell-characteristic genes and—to a lesser extent—of NK-cell-specific genes. Of note, *CD48* mRNA increase was not associated with high or low SARS-CoV-2 viral burden. Unlike *CD48*, mRNA levels of its high-affinity ligand, *2B4*, did not show significant changes when compared with the other lung pathologies studied and with control tissues. An exception was the lungs of patients infected with influenza virus, which showed a decrease in *2B4* mRNA. The expression of *CD48* mRNA in the bronchoalveolar lavage fluid of patients with COVID-19 was reported by Desterke et al.<sup>19</sup> In their study, *CD48* enhancement was related with disease severity and was associated with a specific *CD14-CD16* subpopulation. In our study, we did not find a particular correlation between *CD48* mRNA and monocyte and/or macrophage markers in the lungs.

Similarly to GEP, by analyzing *CD48* protein levels, we found that *CD48* $\pm$  immune cell levels were also significantly increased in patients with COVID-19. Moreover, SARS-CoV-2-affected lungs were characterized by *CD48* $\pm$  intra-alveolar lymphocytosis, even though both COVID-19 and non-COVID-19 DAD displayed similar numbers of intra-alveolar immune cells. A previous report has shown no differences in lymphocyte infiltration in the lungs of individuals infected with SARS-CoV-2 and those infected with influenza. In our study, no *CD48* $\pm$  lymphocytes were found in the intra-alveolar space of patients infected with influenza.<sup>20</sup> Therefore, *CD48* may be of specific importance in COVID-19. This is further supported by the data obtained from complementary studies performed in peripheral blood samples of patients with COVID-19. Interestingly, individuals infected with SARS-CoV-2 showed significant increases in m*CD48* on most peripheral blood leukocytes compared with control samples, regardless of disease severity. These increases may be due to the augmented levels of interferon  $\gamma$  that have been reported in patients with COVID-19,<sup>21</sup> which may upregulate *CD48* expression.<sup>22</sup> Notably, viral infections influence m*CD48* expression. For instance, m*CD48* is elevated on B cells obtained from patients with mononucleosis,<sup>23</sup> whereas on peripheral blood *CD4*-expressing (*CD4* $\pm$ ) T cells from patients infected with T-lymphotropic virus 1, it is decreased,<sup>24</sup> and on NK cells of patients infected with herpes simplex virus, it remains stable.<sup>25</sup> Furthermore, m*CD48* expression has been reported to be elevated in *CD4* $\pm$  T cells infected in vitro with the human immunodeficiency virus.<sup>26</sup> To the best of our knowledge, this is the first report that shows induction of m*CD48* levels on peripheral blood leukocytes after a respiratory viral infection. Interestingly, we have previously shown that m*CD48* levels are altered in other, non-COVID-19

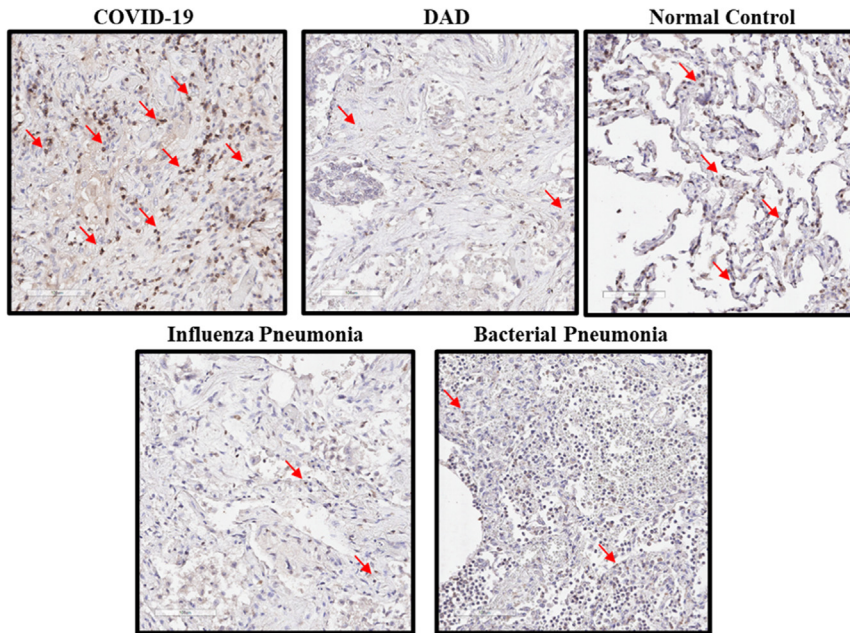
A.



B.



C.



D.

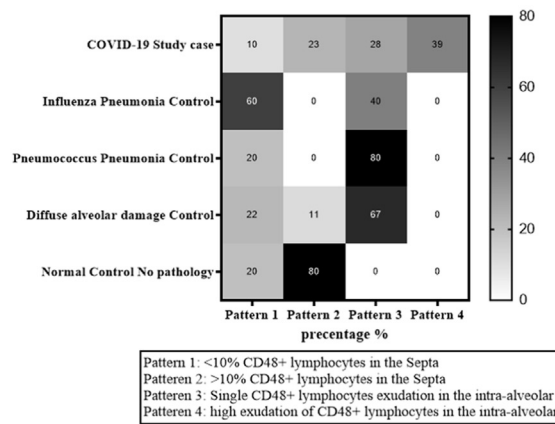


**Figure 2.** GEP and IHC staining of postmortem lung specimens of patients with COVID-19, of other pathologies, and healthy tissue: (A) GEP showed gene expression differences between COVID-19 samples and other pathologies (DAD; influenza pneumonia; patients with hypertensive disease; normal lungs; and bacterial pneumonia) as presented by the heatmap; (B) *CD48* mRNA levels in COVID-19 samples compared with individuals and combined controls as shown in A. (C) Representative images of CD48 tissue staining of either COVID-19, DAD, healthy tissue, influenza pneumonia, or pneumococcus pneumonia, X40; (D) A semiquantitative analysis of the different patterns shown in C. COVID-19, coronavirus disease 2019; DAD, diffuse alveolar damage; GEP, gene expression programming; IHC, immunohistochemistry; mRNA, messenger RNA.

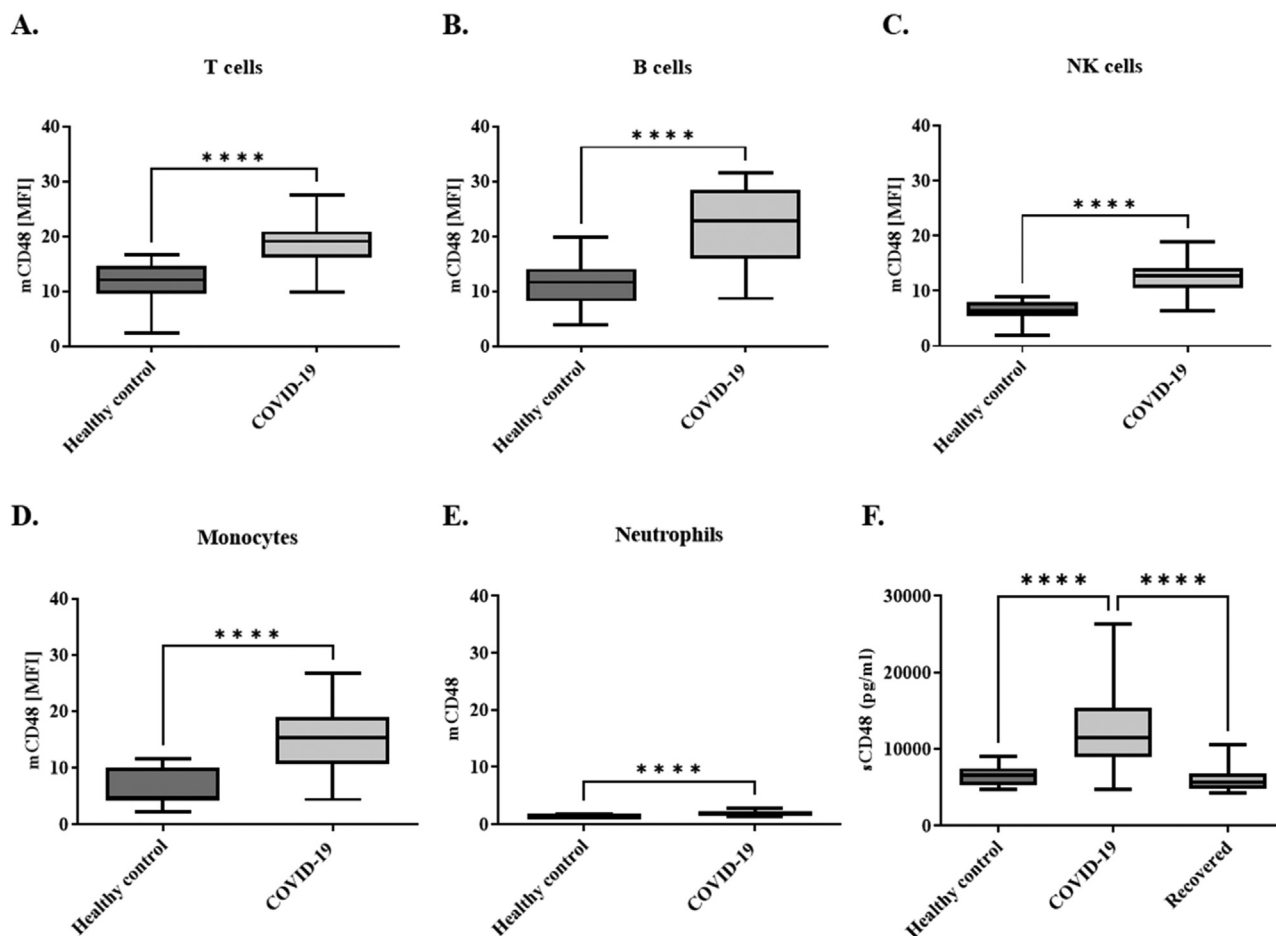


**Figure 3.** Membrane-associated and soluble CD48 levels of patients with COVID-19 and healthy controls: mCD48 expression on (A) T cells; (B) B cells; (C) NK cells; (D) Monocytes; (E) Neutrophils from patients with COVID-19 and HCs identified by staining with their specific cell surface markers; (F) sCD48 levels in the sera of patients with COVID-19, HCs, and individuals recovered from COVID-19; data are shown as the mean ± SEM. Asterisk denotes  $P < .05$ , double asterisks denote  $P < .01$ , triple asterisks denote  $P < .001$ , four asterisks denote  $P < .0001$ . COVID-19, coronavirus disease 2019; HCs, healthy controls; mCD48, membrane-bound CD48; sCD48, soluble CD48.

**Table 2**  
mCD48 Expression Levels (MFI) on Peripheral Blood Leukocytes of Age-matched Patients With Active COVID-19 and Healthy Controls

Individuals' age, mCD48 expression levels, individuals' number	Healthy controls	COVID-19
Age (mean)	4 ± 54	4 ± 57
mCD48 on NK cells (mean)	0.5 ± 6	1 ± 13
mCD48 on T cells (mean)	1 ± 12	1 ± 18
mCD48 on B cells (mean)	1 ± 12	2 ± 22
mCD48 on monocytes (mean)	1 ± 7	1 ± 14
mCD48 on neutrophils (mean)	0 ± 1.44	0 ± 1.88
n	15	19

Abbreviations: COVID-19, coronavirus disease 2019; mCD48, membrane-bound CD48; n, number.  
NOTE. Data presented as mean ± SEM.

**Table 3**  
sCD48 Levels in the Sera of Age-Matched Patients With Active COVID-19 or Patients Recovered From COVID-19 and Healthy Controls

sCD48 levels, individuals' age and number	Healthy controls	COVID-19 all	Mild	Moderate	Severe	Critical	Recovered
sCD48 pg/mL (mean)	258 ± 6555	546 ± 12,511	1303 ± 11,859	8567 ± 9690	751 ± 13,882	1580 ± 12,056	398 ± 5997
Age (mean)	3 ± 62	2 ± 63	6 ± 56	4 ± 54	2 ± 67	2 ± 69	3 ± 49
n	24	88	18	14	42	14	16

Abbreviations: COVID-19, coronavirus disease 2019; n, number; sCD48, soluble CD48.  
NOTE. Data presented as mean ± SEM.

–related lung disorders, such as asthma<sup>10</sup> and chronic obstructive pulmonary disease (COPD) (Berkmann N and Levi-Schaffer F, unpublished data, 2022). Because viral infections are common in these conditions,<sup>8,9</sup> their crosstalk with mCD48 expression underlying respiratory pathologies needs careful consideration.

Similar to mCD48, sCD48 levels were significantly higher in the sera of patients with COVID-19. Interestingly, these increases were independent of disease severity and returned to baseline levels in patients who recovered. It must be noted that the effect of treatment on sCD48 was evaluated in patients with mild-to-moderate disease because patients who were untreated were available only in this group. However, no significant difference was found between patients who were treated and those who were untreated. This suggests that, as in asthma, in COVID-19, oral corticosteroids do not



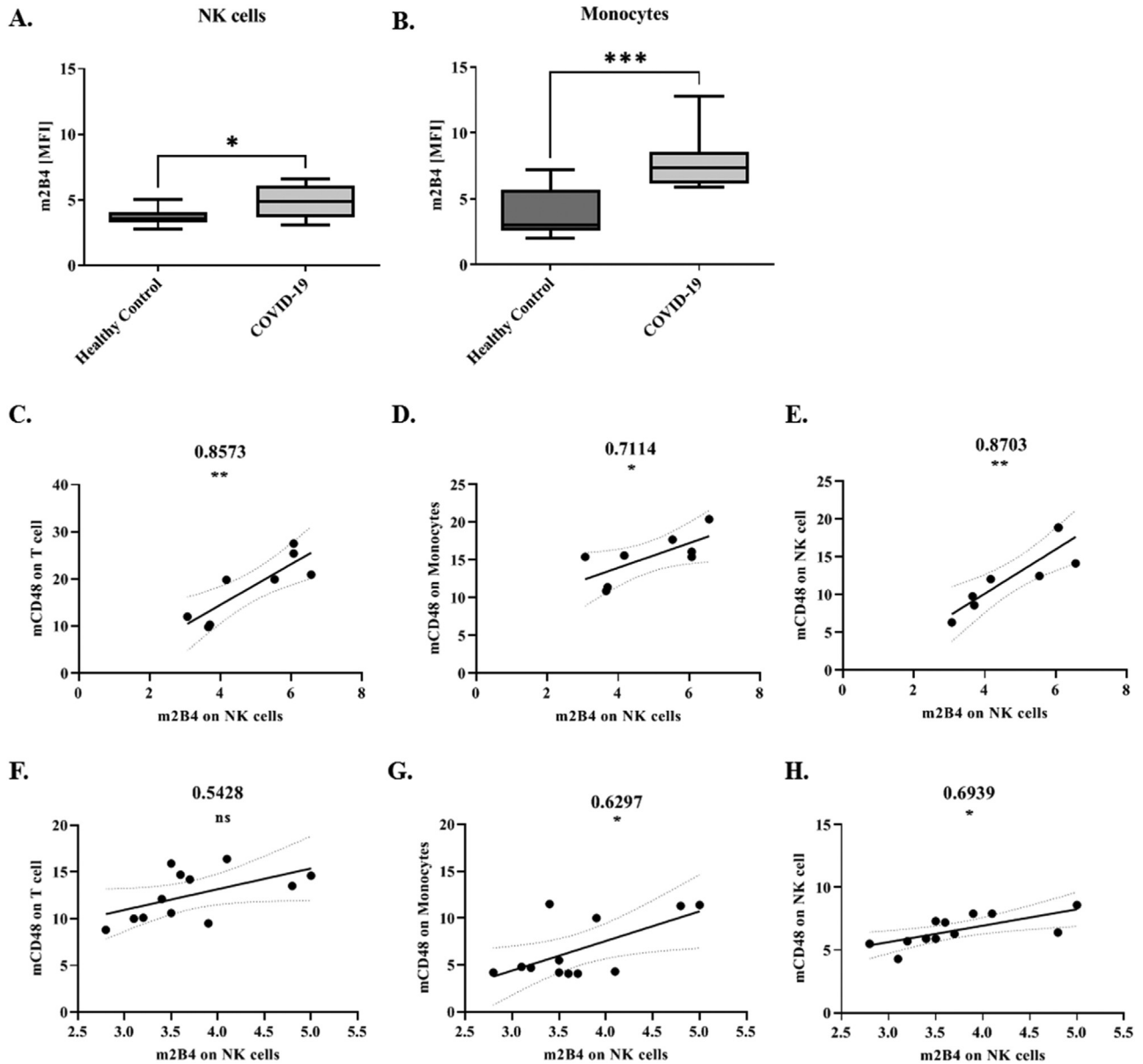


**Figure 4.** Membrane-associated 2B4 levels of patients with COVID-19 and healthy controls: m2B4 expression on (A) NK cells; (B) Monocytes from patients with COVID-19 and HCs identified by staining with their specific cell surface markers. Data are shown as the mean  $\pm$  SEM. Asterisk denotes  $P < .05$ , double asterisks denote  $P < .01$ , triple asterisks denote  $P < .001$ , four asterisks denote  $P < .0001$ . Pearson correlation analysis between m2B4 on NK cells and mCD48 on (C) T cells; (D) Monocytes; and (E) NK cells of patients with COVID-19 or (F) T cells; (G) Monocytes; and (H) NK cells of HCs. COVID-19, coronavirus disease 2019; HCs, healthy controls; m2B4, membrane-bound 2B4.

affect CD48. Furthermore, because no differences in sCD48 levels were found between blood samples collected during the 3 different waves (data not shown), we may posit that sCD48 release is not affected by the different SARS-CoV-2 variants and variations in the treatment strategy.

Considering that IL-6 and CRP are accepted markers of COVID-19 severity, we showed that IL-6 and CRP increases were dependent on the severity of the disease in our samples. However, sCD48 levels significantly increased even in patients with mild disease, and they were significantly correlated with IL-6 and CRP levels in this cohort. This finding identifies sCD48 release as a potential indicator of inflammation. We have previously reported that sCD48 is a decoy receptor for both m2B4 and *Staphylococcus aureus* enterotoxin B (SEB) on human peripheral blood eosinophils and in mouse *Staphylococcus aureus* enterotoxin B-induced peritonitis.<sup>11</sup> In addition, CMV has been reported to produce an sCD48 homologue named A43, which inhibits NK-cell function through binding to m2B4, thus allowing CMV to escape the immune response.<sup>27</sup> It can therefore be

postulated that sCD48 in patients with COVID-19 might play a role as regulator of the immune response by masking its ligand m2B4. However, further investigations are needed regarding this putative functional response. In addition, m2B4 expression levels on both NK cells and monocytes were significantly higher in COVID-19 peripheral blood samples than in their healthy counterparts. Similar increases of m2B4 expression were observed in in vitro experiments in which NK cells were incubated with influenza virus. Interestingly, patients vaccinated against influenza also displayed an increase of m2B4-expressing NK cells.<sup>28</sup> Moreover, we found a positive correlation at the protein level between m2B4 on NK and mCD48 on monocytes, NK cells, and T cells in peripheral blood. Of note, the correlation between m2B4 on NK cells and mCD48 on T cells was found only on patient cells and not on those of healthy individuals. In contrast, the positive correlation between m2B4 on NK cells and mCD48 on monocytes and NK cells was found in both patients with COVID-19 and healthy controls. Finally, the significance in disease symptomatology of the negative correlation between sCD48 levels and the number of

platelets in peripheral blood samples of patients with COVID-19 needs to be carefully investigated, particularly regarding the vasculature pathology underlying the disease.<sup>29–31</sup>

This work presents novel molecular characteristics of SARS-CoV-2 –induced disease. The increases in mCD48 on the peripheral blood lymphocytes, which is paralleled by the lung-infiltrating lymphocytes, along with the increased levels of sCD48 in the serum of patients with COVID-19, are indicative of a central role for CD48 in the inflammatory response during SARS-CoV-2 infection. Moreover, because sCD48 levels are increased in patients with mild symptoms and remain high even in patients who are critically ill, the results of this study may provide the lead for the prospective evaluation of CD48 as an indicator of symptomatic SARS-CoV-2 infection.

### Acknowledgments

The authors thank Prof Ora Schueler-Furman (Department of Microbiology and Molecular Genetics, Institute for Medical Research Israel-Canada, Faculty of Medicine, The Hebrew University of Jerusalem) for helpful discussion, Dr Hadas Segev-Yekutieli (The Core Research Facility, The Faculty of Medicine, The Hebrew University of Jerusalem) who provided advice on the FC analysis and technical help, and all the donors who donated the blood for the study.

### Supplementary Data

Supplementary data related to this article can be found at <https://doi.org/10.1016/j.anaai.2022.10.009>

### References

- Pahima H, Puzzovio PG, Levi-Schaffer F. 2B4 and CD48: A powerful couple of the immune system. *Clin Immunol*. 2019;204:64–68.
- Smith GM, Biggs J, Norris B, Anderson-Stewart P, Ward R. Detection of a soluble form of the leukocyte surface antigen CD48 in plasma and its elevation in patients with lymphoid leukemias and arthritis. *J Clin Immunol*. 1997;17(6):502–509.
- Katsuura M, Shimizu Y, Akiba K, Kanazawa C, Mitsui T, Sendo D, et al. CD48 expression on leukocytes in infectious diseases: flow cytometric analysis of surface antigen. *Acta Paediatr Jpn*. 1998;40(6):580–585.
- Pérez-Carmona N, Farré D, Martínez-Vicente P, Terhorst C, Engel P, Angulo A. Signaling lymphocytic activation molecule family receptor homologs in New World monkey cytomegaloviruses. *J Virol*. 2015;89(22):11323–11336.
- Wiersinga WJ, Rhodes A, Cheng AC, Peacock SJ, Prescott HC. Pathophysiology, transmission, diagnosis, and treatment of coronavirus disease 2019 (COVID-19): a review. *JAMA*. 2020;324(8):782–793.
- Bösmüller H, Matter M, Fend F, Tzankov A. The pulmonary pathology of COVID-19. *Virchows Arch*. 2021;478(1):137–150.
- Herold T, Wörnle M, Schelling J. [COVID-19 in GP practice and emergency rooms]. *Dtsch Med Wochenschr*. 2020;145(15):1080–1085.
- Scherzer R, Grayson MH. Heterogeneity and the origins of asthma. *Ann Allergy Asthma Immunol*. 2018;121(4):400–405.
- Vinoli C, Vogelmeier CF. Exacerbations of COPD. *Eur Respir Rev*. 2018;27(147):170103.
- Gangwar RS, Minai-Fleminger Y, Seaf M, Gutgold A, Shikotra A, Barber C, et al. CD48 on blood leukocytes and in serum of asthma patients varies with severity. *Allergy*. 2017;72(6):888–895.
- Gangwar RS, Levi-Schaffer F. sCD48 is anti-inflammatory in Staphylococcus aureus Enterotoxin B-induced eosinophilic inflammation. *Allergy*. 2016;71(6):829–839.
- Breuer O, Gangwar RS, Seaf M, Barhoum A, Kerem E, Levi-Schaffer F. Evaluation of soluble CD48 levels in patients with allergic and nonallergic asthma in relation to markers of Type 2 and non-type 2 immunity: an observational study. *J Immunol Res*. 2018;2018:4236263.
- Tzankov A, Bhattacharyya S, Kotlo K, Tobacman JK. Increase in chondroitin sulfate and decline in arylsulfatase B may contribute to pathophysiology of COVID-19 respiratory failure. *Pathobiology*. 2022;89:81–91.
- Menter T, Haslbauer JD, Nienhold R, Savic S, Hopfer H, Deigendesch N, et al. Post-mortem examination of COVID-19 patients reveals diffuse alveolar damage with severe capillary congestion and variegated findings in lungs and other organs suggesting vascular dysfunction. *Histopathology*. 2020;77(2):198–209.
- World Health Organization. *Clinical Management of COVID-19: Interim Guidance*, 27 May 2020. Geneva, Switzerland: World Health Organization; 2020.
- Haslbauer JD, Zinner C, Stalder AK, Schneeberger J, Menter T, Bassetti S, et al. Vascular damage, thromboinflammation, plasmablast activation, T-cell dysregulation and pathological histiocytic response in pulmonary draining lymph nodes of COVID-19. *Front Immunol*. 2021;12:763098.
- Reinhold A, Tzankov A, Matter MS, Mihic-Probst D, Scholl HPN, Meyer P. Ocular pathology and occasionally detectable intraocular severe acute respiratory syndrome coronavirus-2 RNA in five fatal coronavirus disease-19 cases. *Ophthalm Res*. 2021;64(5):785–792.
- Zenarruzabeitia O, Gabirel AP, Iñigo T, Ane O, Raquel PG, Iratxe S B, et al. T cell activation, highly armed cytotoxic cells and a shift in monocytes CD300 receptors expression is characteristic of patients with severe COVID-19. *Front Immunol*. 2021;12:655934.
- Desterke C, Turhan AG, Bennaceur-Griscelli A, Griscelli F. PPAR $\gamma$  cistrome repression during activation of lung monocyte-macrophages in severe COVID-19. *iScience*. 2020;23(10):101611.
- Ackermann M, Verleden SE, Kuehnel M, Haverich A, Welte T, Laenger F, et al. Pulmonary vascular endothelialitis, thrombosis, and angiogenesis in Covid-19. *N Engl J Med*. 2020;383(2):120–128.
- Akbari H, Tabrizi R, Lankarani KB, Aria H, Vakili S, Asadian F, et al. The role of cytokine profile and lymphocyte subsets in the severity of coronavirus disease 2019 (COVID-19): a systematic review and meta-analysis. *Life Sci*. 2020;258:118167.
- Tissot C, Rebouissou C, Klein B, Mechti N. Both human alpha/beta and gamma interferons upregulate the expression of CD48 cell surface molecules. *J Interferon Cytokine Res*. 1997;17(1):17–26.
- Thorley-Lawson DA, Schooley RT, Bhan AK, Nadler LM. Epstein-Barr virus superinduces a new human B cell differentiation antigen (B-LAST 1) expressed on transformed lymphoblasts. *Cell*. 1982;30(2):415–425.
- Ezinne CC, Yoshimitsu M, White Y, Arima N. HTLV-1 specific CD8+ T cell function augmented by blockade of 2B4/CD48 interaction in HTLV-1 infection. *PLoS One*. 2014;9(2):e87631.
- Lenart M, Kluczevska A, Szaflarska A, Rutkowska-Zapała M, Wąsik M, Ziemiańska-Pięta A, et al. Selective downregulation of natural killer activating receptors on NK cells and upregulation of PD-1 expression on T cells in children with severe and/or recurrent herpes simplex virus infections. *Immunobiology*. 2021;226(3):152097.
- Tremblay-McLean A, Bruneau J, Lebouché B, Lisovsky I, Song R, Bernard NF. Expression profiles of ligands for activating natural killer cell receptors on HIV infected and uninfected CD4<sup>+</sup> T cells. *Viruses*. 2017;9(10):295.
- Martínez-Vicente P, Farré D, Sánchez C, Alcami A, Engel P, Angulo A. Subversion of natural killer cell responses by a cytomegalovirus-encoded soluble CD48 decoy receptor. *PLoS Pathog*. 2019;15(4):e1007658.
- Jost S, Reardon J, Peterson E, Poole D, Bosch R, Alter G, et al. Expansion of 2B4<sup>+</sup> natural killer (NK) cells and decrease in NKp46<sup>+</sup> NK cells in response to influenza. *Immunology*. 2011;132(4):516–526.
- Wool GD, Miller JL. The impact of COVID-19 disease on platelets and coagulation. *Pathobiology*. 2021;88(1):15–27.
- Rohlfing A-K, Rath D, Geisler T, Gawaz M. Platelets and COVID-19. *Hamostaseologie*. 2021;41(5):379–385.
- Barale C, Melchionda E, Morotti A, Russo I. Prothrombotic phenotype in COVID-19: focus on platelets. *Int J Mol Sci*. 2021;22(24):13638.

## Supplementary Data

**eTable 1**  
Comorbidities Characteristics of COVID-19 Autopsies

Basel patient number (Y/N)	Hypertension	Cancer	Diabetes	Obesity	Chronic respiratory disease		Chronic renal disease
	(Y/N)	(Y/N)	(Y/N)	(Y/N) (BMI)	(Y/N)	Specify disease	(Y/N)
B-1	Y	N	Not available	Y	N	Not available	Acute (AKIN2) on chronic
B-2	Y	Y	Type II	Y	Y	Sleep apnea	N
B-3	Y	N	Not available	N	N	Not available	Acute (AKIN1)
B-4	Y	N	Type II	Y	Y	Sleep apnea, smoker	Acute (AKIN1) on chronic
B-5	Y	N	Not available	Y	N	Former smoker, OSAS	Acute (AKIN3) on chronic
B-6	Y	Y	Type II	Y	Y	Former smoker, COPD, wedge resection of lung	Acute (AKIN3) on chronic
B-7	Y	N	Not available	Y	N	Former smoker	Acute (AKIN1)
B-8	N	N	Not available	N	N	Not available	Acute (AKIN3)
B-9	N	N	Not available	Y	N	Not available	N
B-10	Y	N	Not available	Y	N	Former smoker	Acute (AKIN3) on chronic
B-11	Y	N	Not available	Y	N	Not available	Acute (AKIN3)
B-12	N	N	Not available	Y	N	No	Acute renal disease
B-13	Y	N	Type II	Y	Y	Not available	Renal insufficiency
B-14	N	N	N	Y	Y	ARDS	Chronic renal disease AKIN3
B-15	Not available	Not available	Not available	Not available	Not available	Not available	Not known
B-16	Y	N	Type II	Not available	Y	Sleep apnea, former smoker, COPD	N
B-17	N	N	Type II	Y	N	No	N
B-18	Y	N	N	Y	Y	Former smoker, severe OSAS	N
B-19	Y	N	Type II	Not available	Y	Not known	Acute renal disorder AKIN1
B-20	Y	N	Type II	Y	Y	Former smoker, (90 py), COPD, severe OSAS	Renal insufficiency AKIN1
B-21	Y	N	N	Y	N	Not available	Acute renal failure
B-22	Y	Y	N	Y	N	Not available	Chronic renal failure
B-23	Y	N	N	Y	N	Not available	Chronic kidney insufficiency KDIGO G3b
B-24	Y	Y	Type II	N	N	Not available	Acute renal insufficiency
B-25	Not available	Not available	N	Y	Not available	Not available	Acute renal insufficiency AKIN2
B-26	Not available	Not available	N	Y	Not available	Not available	Chronic and acute renal insufficiency
B-27	Y	Not available	N	Y	Not available	Not available	Chronic and acute renal insufficiency
B-28	Y	N	N	N	N	Not available	Acute renal insufficiency AKIN2

Abbreviations: AKIN, acute kidney injury network; ARDS, acute respiratory distress syndrome; COPD, chronic obstructive pulmonary disease; KDIGO, kidney disease improving global outcomes; N, no; OSAS, Obstructive Sleep Apnea Syndrome; py, pack-years smoked; Y, yes.

**eTable 2**  
Demographic and Clinical Characteristics of Patients With Active COVID-19

Patient ID	Age	Sex	Mechanical ventilation	ICU admission	Outcome	Clinical stat during sampling	Swab to sample (d)	IMAGING
P1	73	Male	No	Yes	Recovery	Severe	Not available	Pneumonia
P2	54	Male	No	Yes	Recovery	Severe	1	Pneumonia
P3	59	Male	No	No	Recovery	Mild	Not available	Possible pneumonia
P4	33	Male	No	No	Recovery	Moderate	Not available	Pneumonia
P5	30	Female	No	No	Recovery	Mild	8	No pneumonia
P6	76	Male	No	Yes	Death	Severe	Not available	Pneumonia
P7	71	Male	No	No	Recovery	Moderate	Not available	Pneumonia
P8	54	Male	No	No	Recovery	Mild	1	No pneumonia
P9	69	Male	No	Yes	Death	Severe	Not available	Pneumonia
P10	74	Male	Yes	Yes	Death	Severe	Not available	Pneumonia
P11	79	Female	No	No	Discharge	Severe	3	Pneumonia
P12	77	Female	No	No	Discharge	Mild	2	None
P13	41	Female	No	No	Discharge	Mild	7	None
P14	37	Male	No	No	Discharge	Severe	1	Pneumonia
P15	49	Male	No	No	Discharge	Moderate	10	None
P16	65	Female	No	No	Discharge	Moderate	16	No
P17	51	Male	No	No	Discharge	Severe	13	No
P18	74	Female	No	No	Discharge	Severe	6	No
P19	72	Male	No	No	Death	Critical	10	Possible infection
P20	77	Female	No	No	Discharge	Severe	11	Pneumonia
P21	77	Male	No	No	Discharge	Severe	24	Pneumonia
P22	21	Male	No	No	Discharge	Mild	2	None
P23	62	Male	No	No	Recovery	Mild	6	No pneumonia
P24	65	Male	No	No	Recovery	Moderate	11	Pneumonia
P25	57	Male	No	No	Recovery	Moderate	1	Pneumonia
P26	66	Male	Yes	Yes	Recovery	Critical	20	Pneumonia
P27	71	Male	Yes	Yes	Death	Critical	11	Pneumonia
P28	64	Female	No	No	Recovery	Moderate	3	Pneumonia
P29	51.8	Male	No	No	Recovery	Severe	1	Pneumonia
P30	47	Male	No	No	Recovery	Moderate	6	Pneumonia

(continued)

Table 2 (Continued)

Patient ID	Age	Sex	Mechanical ventilation	ICU admission	Outcome	Clinical stat during sampling	Swab to sample (d)	IMAGING
P31	43	Female	No	No	Recovery	Moderate	9	Pneumonia
P32	74	Male	No	No	Recovery	Severe	2	Pneumonia
P33	34	Male	No	No	Recovery	Moderate	2	Pneumonia
P34	61	Female	Yes	Yes	Recovery	Critical	6	Pneumonia
P35	69	Male	Yes	Yes	Recovery	Critical	13	Pneumonia
P36	77	Male	No	No	Recovery	Moderate	9	Pneumonia
P37	61	Male	No	No	Recovery	Mild	9	No pneumonia
P38	61	Female	No	No	Recovery	Moderate	1	(?) M/P bacterial pneumonia and not COVID-19
P39	23	Female	No	No	Recovery	Mild	1	No pneumonia
P40	77	Male	Yes	Yes	Recovery	Critical	19	Pneumonia
P41	43	Female	No	No	Recovery	Mild	2	No pneumonia
P42	58	Female	No	No	Recovery	Moderate	19	Pneumonia (CT)
P43	64	Male	No	No	Recovery	Moderate	2	Pneumonia + pulmonary emboli (CT)
P44	70	Male	Yes	Yes	Death	Critical	11	Pneumonia
P45	74	Male	No	No	Recovery	Mild	0	No pneumonia
P46	67	Female	Yes	Yes	Recovery	Critical	2	Pneumonia
P47	73	Male	Yes	Yes	Recovery	Severe	4	Pneumonia
P48	44	Male	No	No	Recovery	Moderate	14	Pneumonia
P49	36	Female	No	No	Recovery	Moderate	5	Pneumonia
P50	65	Male	Yes	Yes	Recovery	Severe	3	Pneumonia
P51	61	Male	Yes	Yes	Recovery	Critical	5	Pneumonia
P52	70	Male	Yes	Yes	Death	Severe	7	Pneumonia
P53	80	Female	Yes	Yes	Death	Severe	5	Pneumonia
P54	66	Male	Yes	Yes	Death	Critical	3	Pneumonia
P55	62	Male	Yes	Yes	Recovery	Critical	4	Pneumonia
P56	46	Male	No	No	Recovery	Severe	~ 6 (swab taken a few days before admission)	Pneumonia
P57	92	Female	No	No	Recovery	Mild	2	Pneumonia
P58	44	Male	No	No	Recovery	Severe	4	Pneumonia
P59	94	Female	No	No	Recovery	Severe	1	Pneumonia
P60	74	Male	Yes	Yes	Death	Severe	4	Pneumonia
P61	47	Male	No	No	Recovery	Mild	8	No pneumonia
P62	43	Male	No	No	Recovery	Mild	6	No pneumonia
P63	42	Female	No	No	Recovery	Mild	1	No pneumonia
P64	62	Male	No	No	Recovery	Severe	1	No pneumonia
P65	64	Male	Yes	Yes	Death	Critical	10	Pneumonia
P66	92	Male	Yes	No	Death	Severe	3	Pneumonia
P67	92	Male	No	No	Recovery	Mild	1	No pneumonia
P68	57	Female	No	No	Recovery	Severe	10	Pneumonia
P69	63	Male	No	No	Recovery	Severe	2	No pneumonia
P70	71	Male	No	No	Recovery	Mild	1	No pneumonia
P71	66	Male	No	No	Recovery	Mild	1	No pneumonia
P72	73	Male	No	No	Death	Mild	1	Pneumonia
P73	19	Female	No	No	Recovery	Mild	1	No pneumonia
P74	43	Female	No	No	Recovery	Mild	8	No pneumonia
P75	87	Female	No	No	Recovery	Moderate	0	Pneumonia
P76	93	Female	No	No	Recovery	Mild	2	Pulmonary emboli (CT)
P77	87	Male	No	No	Recovery	Mild	2	No pneumonia
P78	57	Male	No	No	Recovery	Moderate	4	No pneumonia
P79	99	Female	No	No	Death	Severe	1	Pneumonia
P80	88	Female	No	No	Death	Severe	8	Pneumonia
P81	52	Female	Yes	No	Death	Severe	0	Pneumonia
P82	87	Male	No	No	Death	Severe	1	Pneumonia
P83	80	Female	Yes	No	Death	Severe	9	Pneumonia
P84	87	Female	No	No	Death	Severe	1	Pneumonia
P85	72	Female	No	No	Death	Severe	8	Pneumonia
P86	88	Female	No	No	Death	Severe	2	Pneumonia
P87	89	Male	Yes	Yes	Recovery	Critical	13	Bilateral infiltrates
P88	78	Female	No	No	Recovery	Severe	1	Rt lung consolidation
P89	50	Female	No	No	Recovery	Severe	10	Rt lobar consolidation
P90	53	Female	No	No	Recovery	Severe	3	Bilateral patchy infiltrates
P91	49	Male	No	No	Recovery	Severe	7	Bilateral patchy infiltrates
P92	48	Female	No	Yes	Recovery	Mild	1	Not available
P93	42	Female	Yes	Yes	Recovery	Severe	2	Diffuse bilateral ground-glass
P94	60	Female	Yes	Yes	Recovery	Severe	1	Diffuse bilateral ground-glass
P95	60	Female	Yes	Yes	Recovery	Severe	8	Diffuse bilateral ground-glass
P96	34	Male	Yes	Yes	Recovery	Moderate	1	Diffuse bilateral ground-glass
P97	69	Male	Yes	Yes	Recovery	Severe	0	Diffuse bilateral ground-glass
P98	64	Female	Yes	Yes	Recovery	Severe	1	Diffuse bilateral ground-glass
P99	69	Male	Yes	Yes	Recovery	Severe	2	Diffuse bilateral ground-glass
P100	49	Female	No	Yes	Recovery	Moderate	1	Diffuse bilateral ground-glass
P101	65	Male	Yes	Yes	Recovery	Severe	1	Diffuse bilateral ground-glass
P102	50	Male	No	Yes	Recovery	Moderate	2	Diffuse bilateral ground-glass
P103	49	Male	Yes	Yes	Recovery	Severe	1	Diffuse bilateral ground-glass
P104	42	Female	No	Yes	Recovery	Moderate	0	TUS (pregnant)

(continued)



**eTable 2** (Continued)

Patient ID	Age	Sex	Mechanical ventilation	ICU admission	Outcome	Clinical stat during sampling	Swab to sample (d)	IMAGING
P105	42	Male	Yes	Yes	Recovery	Severe	4	Diffuse bilateral ground-glass
P106	70	Female	Yes	Yes	Recovery	Severe	0	Diffuse bilateral ground-glass
P107	48	Male	Yes	Yes	Recovery	Severe	0	Lobar pneumonia
P108	86	Male	Yes	Yes	Death	Severe	1	Diffuse bilateral ground-glass
P109	58	Female	Yes	Yes	Recovery	Severe	0	Diffuse bilateral ground-glass
P110	85	Female	Yes	Yes	Recovery	Severe	1	Pneumonia+ fibrosis
P111	85	Female	Yes	Yes	Recovery	Mild	0	Pneumonia+ fibrosis

Abbreviations: CT, computed tomography; ICU, intensive care unit; rt, right; TUS, transabdominal ultrasound.

**eTable 3**

List of Drugs Administered to the Israeli and Italian Patients With Active Disease

Patient ID	Any corticosteroids	Remdesivir	Hydroxychloroquine	Low molecular weight heparin	Hyperimmune plasma	Intravenous immunoglobulin	Tocilizumab	Baricitinib	Immunosuppressant	Azidothymidine
P1	Yes	Yes	No	Yes	No	No	No	No	No	No
P2	Yes	Yes	No	Yes	No	No	No	No	No	No
P3	No	No	No	Yes	No	No	No	No	No	No
P4	Yes	No	No	No	No	No	No	No	No	No
P5	Yes	No	No	No	No	No	No	No	No	No
P6	No	Yes	No	Yes	No	No	No	No	No	No
P7	Yes	No	No	Yes	No	No	No	No	No	No
P8	Yes	No	No	No	No	No	No	No	Yes	No
P9	Yes	No	No	Yes	No	No	No	No	No	No
P10	Yes	Yes	No	Yes	No	No	No	No	No	No
P11	Yes	No	No	Yes	No	No	No	No	No	No
P12	Yes	No	No	Yes	No	No	No	No	Yes	No
P13	Not available	Not available	Not available	Not available	Not available	Not available	Not available	Not available	Not available	Not available
P14	Yes	No	No	Yes	No	No	No	No	No	No
P15	Yes	No	No	Yes	No	No	No	No	No	No
P16	Yes	No	No	Yes	No	No	No	No	No	No
P17	Yes	No	No	Yes	No	No	No	No	No	No
P18	Yes	No	No	No	No	Yes	No	No	No	No
P19	Yes	No	No	Yes	No	No	No	No	No	No
P20	Yes	No	No	Yes	No	No	No	No	No	No
P21	No	No	No	Yes	No	No	No	No	No	No
P22	No	No	No	No	No	No	No	No	No	No
P23	Yes	No	No	No	No	No	No	No	No	No
P24	No	No	Yes	No	No	No	No	No	No	Yes
P25	No	No	Yes	No	No	No	No	No	No	Yes
P26	Yes	No	Yes	Yes	No	No	No	No	No	No
P27	Yes	No	Yes	Yes	No	No	No	No	No	No
P28	No	No	No	Yes	No	No	No	No	No	No
P29	No	No	Yes	Yes	No	No	No	No	No	Yes
P30	No	No	No	Yes	No	No	No	No	No	No
P31	No	No	No	No	No	No	No	No	No	No
P32	No	No	Yes	Yes	No	No	No	No	No	Yes
P33	No	No	No	No	No	No	No	No	No	No
P34	No	No	Yes	No	No	No	No	No	No	No
P35	Yes	No	No	Yes	No	No	No	No	No	No
P36	No	No	No	No	No	No	No	No	No	No
P37	No	No	No	No	No	No	No	No	No	No
P38	No	No	No	No	No	No	No	No	No	No
P39	No	No	No	No	No	No	No	No	No	No
P40	No	No	Yes	Yes	No	No	No	No	No	No
P41	No	No	No	No	No	No	No	No	No	No
P42	No	No	No	Yes	No	No	No	No	No	No
P43	No	No	No	Yes	No	No	No	No	No	No
P44	Yes	No	No	Yes	No	No	No	No	No	No
P45	No	No	No	No	No	No	No	No	No	No
P46	Yes	Yes	No	No	No	No	No	No	Yes	No
P47	Yes	Yes	No	Yes	No	No	No	No	No	No
P48	No	No	No	Yes	No	No	No	No	No	No
P49	Yes	No	No	Yes	No	No	No	No	No	No
P50	Yes	Yes	No	Yes	No	No	No	No	No	No
P51	Yes	Yes	No	Yes	No	No	No	No	No	No
P52	Yes	Yes	No	Yes	No	No	No	No	No	No

(continued)

eTable 3 (Continued)

Patient ID	Any corticosteroids	Remdesivir	Hydroxychloroquine	Low molecular weight heparin	Hyperimmune plasma	IntraveNous immunoglobulin	Tocilizumab	Baricitinib	Immunosuppressant	Azidothymidine
P53	Yes	No	No	Yes	No	No	No	No	No	Yes
P54	Yes	No	No	No	No	No	No	No	No	No
P55	Yes	Yes	No	Yes	No	No	No	No	No	No
P56	Yes	Yes	No	Yes	No	No	No	No	No	No
P57	No	No	No	Yes	No	No	No	No	No	No
P58	Yes	No	No	Yes	Yes	No	No	No	No	No
P59	No	No	Yes	No	No	No	No	No	No	No
P60	Yes	Yes	No	No	No	No	No	No	No	No
P61	No	No	No	No	No	No	No	No	No	No
P62	No	No	No	No	No	No	No	No	No	No
P63	No	No	No	No	No	No	No	No	No	No
P64	No	No	Yes	Yes	No	No	No	No	No	No
P65	Yes	Yes	No	No	No	No	No	No	No	No
P66	Yes	No	No	Yes	No	No	No	No	No	No
P67	No	No	No	Yes	No	No	No	No	No	No
P68	Yes	No	No	Yes	Yes	No	No	No	No	No
P69	Yes	No	No	Yes	No	No	No	No	No	No
P70	Yes	No	No	Yes	No	No	No	No	No	No
P71	No	No	No	Yes	No	No	No	No	No	No
P72	No	No	No	Yes	No	No	No	No	No	No
P73	No	No	No	No	No	No	No	No	No	No
P74	No	No	No	No	No	No	No	No	No	No
P75	No	No	Yes	Yes	No	No	No	No	No	No
P76	No	No	No	Yes	No	No	No	No	No	No
P77	No	No	No	Yes	No	No	No	No	No	No
P78	No	No	Yes	No	No	No	No	No	No	No
P79	No	No	Yes	Yes	No	No	No	No	No	No
P80	Yes	No	No	Yes	No	No	No	No	No	No
P81	No	No	Yes	Yes	No	No	No	No	No	Yes
P82	No	No	Yes	Yes	No	No	No	No	No	No
P83	Yes	No	No	Yes	No	No	No	No	No	No
P84	Yes	No	No	Yes	No	No	No	No	No	No
P85	Yes	No	No	Yes	No	No	No	No	No	No
P86	Yes	No	No	Yes	No	No	No	No	No	No
P87	Yes	No	No	Not available	Not available	Not available	Not available	Not available	Not available	Not available
P88	Yes	No	No	Not available	Not available	Not available	Not available	Not available	Not available	Not available
P89	Yes	No	No	Not available	Not available	Not available	Not available	Not available	Not available	Not available
P90	Yes	Yes	No	Not available	Not available	Not available	Not available	Not available	Not available	Not available
P91	Yes	Yes	No	Not available	Not available	Not available	Not available	Not available	Not available	Not available
P92	Yes	No	No	Yes	No	No	No	No	No	No
P93	Yes	Yes	No	Yes	No	No	No	Yes	No	No
P94	Yes	No	No	Yes	No	No	No	Yes	No	No
P95	Yes	No	No	Yes	No	No	No	Yes	No	No
P96	Yes	No	No	Yes	No	No	No	Yes	No	No
P97	Yes	No	No	Yes	No	No	No	Yes	No	No
P98	Yes	No	No	Yes	No	Yes	No	No	No	No
P99	Yes	Yes	No	Yes	No	No	No	No	No	No
P100	Yes	No	No	Yes	No	No	No	No	No	No
P101	Yes	No	No	Yes	No	No	No	Yes	No	No
P102	Yes	No	No	Yes	No	Yes	No	No	No	No
P103	Yes	No	No	Yes	No	No	No	Yes	No	No
P104	Yes	No	No	Yes	No	No	No	No	No	No
P105	Yes	Yes	No	Yes	No	No	No	Yes	No	No
P106	Yes	No	No	Yes	No	No	Yes	No	No	No
P107	Yes	No	No	Yes	No	Yes	No	No	No	No
P108	Yes	No	No	Yes	No	No	No	No	No	No
P109	Yes	No	No	Yes	No	Yes	No	Yes	No	No
P110	Yes	No	No	Yes	No	No	No	No	No	No
P111	Yes	No	No	Yes	No	No	No	No	No	No

**eTable 4**  
Demographic Characteristics of Patients Recovered From COVID-19

Patient ID	Age	Sex	Mechanical Ventilation	ICU Admission	Outcome	Clinical Stat During Sampling
R1	35	Male	No	No	Recovery	No active disease
R2	64	Female	No	No	Recovery	No active disease
R3	56	Male	Yes	Yes	Recovery	No active disease
R4	62	Male	No	No	Recovery	No active disease
R5	55	Female	No	No	Recovery	No active disease
R6	58	Female	No	No	Recovery	No active disease
R7	62	Male	No	No	Recovery	No active disease
R8	55	Female	No	No	Recovery	No active disease
R9	44	Female	No	No	Recovery	No active disease
R10	43	Female	No	No	Recovery	No active disease
R11	55	Female	No	No	Recovery	No active disease
R12	28	Female	No	No	Recovery	No active disease
R13	28	Female	No	No	Recovery	No active disease
R14	27	Male	No	No	Recovery	No active disease
R15	27	Female	No	No	Recovery	No active disease
R16	64	Female	No	No	Recovery	No active disease
R17	42	Female	No	No	Recovery	No active disease
R18	63	Female	No	No	Recovery	No active disease

**eTable 5**  
Age, Sex, and Date of Blood Sampling of Healthy Donors

Donor ID	Age at screening	Sex	Blood collection date
H1	64	Female	September 02, 2021
H2	31	Male	December 08, 2020
H3	85	Male	August 04, 2020
H4	54	Male	August 04, 2020
H5	73	Female	August 04, 2020
H6	61	Male	September 13, 2021
H7	56	Female	September 02, 2021
H8	62	Male	September 02, 2021
H9	58	Female	September 02, 2021
H10	41	Female	August 26, 2021
H11	33	Male	August 26, 2021
H12	38	Female	October 07, 2020
H13	48	Female	Not available
H14	80	Male	October 14, 2021
H15	63	Female	October 14, 2021
H16	75	Female	October 14, 2021
H17	60	Male	October 14, 2021
H18	63	Male	February 09, 2021
H19	68	Female	November 14, 2021
H20	82	Male	November 14, 2021
H21	82	Female	November 14, 2021
H22	85	Male	November 14, 2021
H23	Not available	Male	November 22, 2020
H24	65	Male	November 22, 2020
H25	30	Male	December 17, 2020
H26	24	Female	December 17, 2020

**eTable 6**  
Demographic Characteristics of Autopsies With COVID-19 Stained for IHC

Basel number	Basic demographics			Height (cm)	BMI	Hospitalization length	Group (6SEP2020 UPDATE)
	Age	Sex	Weight (Kg)				
B-1	67	F	85	157	35	9	COVID-19 Study case
B-2	85	M	71	164	26	5	COVID-19 Study case
B-3	95	M	64	166	23	3	COVID-19 Study case
B-4	77	M	139	178	44	3	COVID-19 Study case
B-5	66	M	80	165	29	9	COVID-19 Study case
B-6	74	M	91	185	27	3	COVID-19 Study case
B-7	81	F	72	165	26	4	COVID-19 Study case
B-8	71	M	79	180	24	0	COVID-19 Study case
B-9	88	M	76	164	28	2	COVID-19 Study case
B-10	85	M	90	174	30	5	COVID-19 Study case
B-11	58	M	121	161	47	7	COVID-19 Study case
B-12	54	M	110	192	30.0	17	COVID-19 Study case
B-13	75	M	Not available	Not available	27	3	COVID-19 Study case
B-14	53	M	Not available	Not available	49	9	COVID-19 Study case
B-15	94	F	Not available	Not available	Not available	Not available	COVID-19 Study case
B-16	89	M	Not available	Not available	Not available	5	COVID-19 Study case
B-17	61	F	172	122	41	9	COVID-19 Study case
B-18	72	M	Not available	Not available	25	16	COVID-19 Study case
B-19	79	M	Not available	Not available	Not available	16	COVID-19 Study case
B-20	65	M	78	172	26	8	COVID-19 Study case
B-21	71	M	107	173	36	3	COVID-19 Study case
B-22	96	M	73	171	25	18	COVID-19 Study case
B-23	89	F	69	160	27	28	COVID-19 Study case
B-24	84	F	60	158	24	12	COVID-19 Study case
B-25	69	F	89	157	36	38	COVID-19 Study case
B-26	79	M	95	178	30	30	COVID-19 Study case
B-27	91	F	73	158	29	1	COVID-19 Study case
B-28	n.a	M	Not available	169	51.0	14.00	COVID-19 Study case
B-59	80	M	Not available	Not available	27	Not available	Influenza Pneumonia Control
B-60	34	F	Not available	Not available	25	Not available	Influenza Pneumonia Control
B-61	67	F	Not available	Not available	25	Not available	Influenza Pneumonia Control
B-62	82	F	Not available	Not available	34	Not available	Influenza Pneumonia Control
B-63	90	F	Not available	Not available	27	Not available	Influenza Pneumonia Control
B-64	76	F	Not available	Not available	35	Not available	Pneumococcus Pneumonia Control
B-65	86	F	Not available	Not available	29	Not available	Pneumococcus Pneumonia Control
B-66	80	M	Not available	Not available	24	Not available	Pneumococcus Pneumonia Control
B-67	82	M	Not available	Not available	18	Not available	Pneumococcus Pneumonia Control
B-68	66	M	Not available	Not available	21	Not available	Pneumococcus Pneumonia Control
B-51	74	F	Not available	Not available	25	Not available	Diffuse alveolar damage Control
B-69	84	M	Not available	Not available	28	Not available	Diffuse alveolar damage Control
B-70	48	M	Not available	Not available	23	Not available	Diffuse alveolar damage Control
B-71	39	F	Not available	Not available	42	Not available	Diffuse alveolar damage Control
B-72	81	M	Not available	Not available	19	Not available	Diffuse alveolar damage Control
B-73	65	M	Not available	Not available	23	Not available	Diffuse alveolar damage Control
B-74	62	M	Not available	Not available	27	Not available	Diffuse alveolar damage Control
B-75	73	M	Not available	Not available	23	Not available	Diffuse alveolar damage Control
B-76	55	M	Not available	Not available	22	Not available	Diffuse alveolar damage Control
B-31	76	M	Not available	Not available	29	Not available	Normal control No pathology
B-32	96	M	Not available	Not available	30	Not available	Normal control No pathology
B-77	65	M	Not available	Not available	33	Not available	Normal control No pathology
B-78	92	F	Not available	Not available	24	Not available	Normal control No pathology
B-79	82	F	Not available	Not available	36	Not available	Normal control No pathology

BMI, body mass index; COVID-19, coronavirus disease 2019; F, female; IHC, immunohistochemistry; M, male.



**eTable 7**

P Values of COVID-19 Lung Tissues vs Control Diseases

Gene	Overall controls	DAD	Influenza viral pneumonia	Lungs of patients with hypertensive disease	Normal lungs	Bacterial pneumonia
<b>CD48</b>	0.0083 <sup>a</sup>	0.000032 <sup>b</sup>	—	0.068	0.046 <sup>c</sup>	—
<b>CD244</b>	NA	NA	0.00000024 <sup>b</sup>	NA	NA	NA
<b>CD27</b>	NA	NA	—	NA	NA	NA
<b>CD3G</b>	0.024 <sup>c</sup>	0.084	—	0.038 <sup>c</sup>	—	—
<b>CD3E</b>	—	—	—	—	—	—
<b>CD3D</b>	—	NA	—	NA	NA	NA
<b>CD8A</b>	—	0.024 <sup>c</sup>	—	—	—	—
<b>CD4</b>	—	—	—	—	—	—
<b>CD160</b>	NA	NA	NA	NA	NA	NA
<b>CD247</b>	0.011 <sup>c</sup>	NA	NA	NA	NA	NA
<b>CD2</b>	0.0027 <sup>a</sup>	< 0.050 <sup>c</sup>	—	0.041 <sup>c</sup>	< 0.050 <sup>c</sup>	—
<b>NCAM1</b>	NA	NA	—	NA	NA	NA
<b>NKG7</b>	—	—	0.031 <sup>c</sup>	—	—	—
<b>MS4A1</b>	—	NA	—	NA	NA	NA
<b>CD19</b>	NA	NA	NA	NA	NA	NA
<b>PAX5</b>	NA	NA	—	NA	NA	NA
<b>CD163</b>	< 0.10	—	—	0.083	0.000000189 <sup>b</sup>	—
<b>CEACAM8</b>	—	NA	—	—	—	0.071
<b>IL6</b>	0.0039 <sup>a</sup>	—	0.059	0.043 <sup>c</sup>	—	0.00050 <sup>d</sup>

NA: No test owing to outlier counts.

Abbreviations: DAD, diffuse alveolar damage; NA, not available.

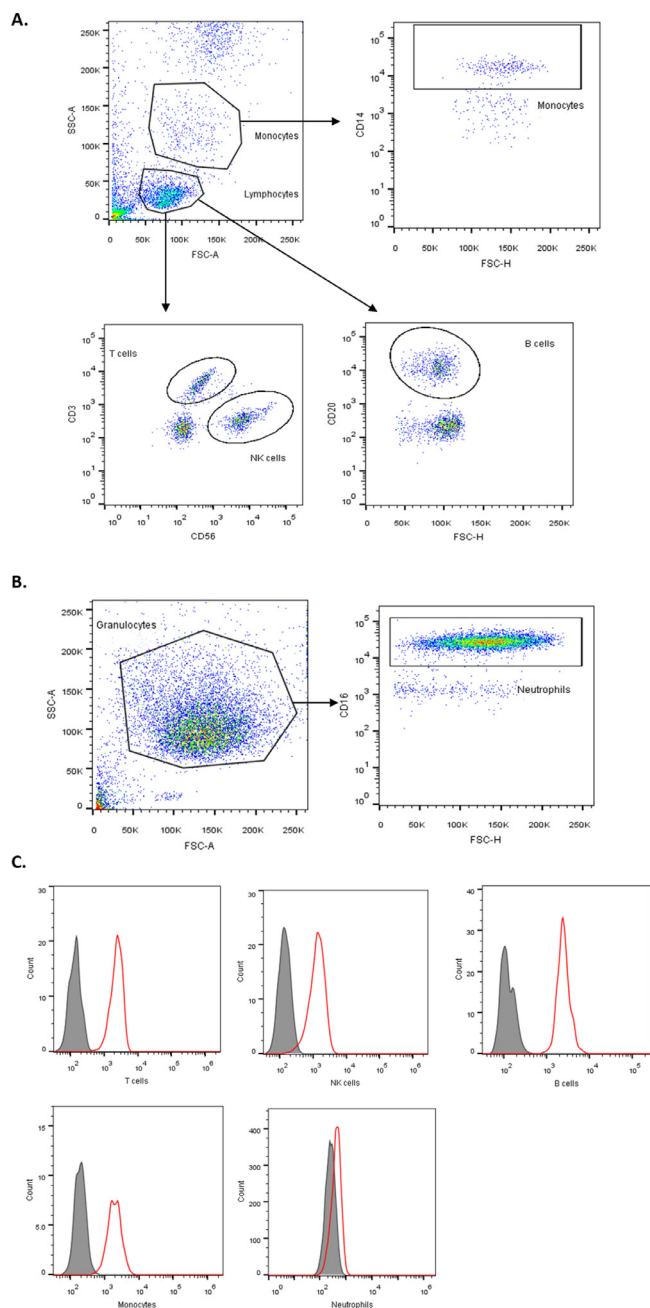


**Figure 1.** Gating and identification of leucocytes from peripheral blood by flow cytometry: (A) Peripheral blood leucocytes were first separated by their physical parameters (FSC and SSC). Lymphocytes and mononuclear cells were identified and gated. From the mononuclear cells gate, monocytes (CD14+) were identified; from the lymphocytes gate, B cells (CD20+), T cells (CD56-/CD3+), and NK cells (CD56+/CD3-) were identified. (B) Granulocytes were first separated by their physical parameters (FSC and SSC). Neutrophils (CD16+) were then identified from the granulocyte population. (C) Representative histogram of CD48 and isotype control intensity on each cell type. The shaded gray histograms represent isotype-matched control, and red open histograms show the specific-CD48 expression on the different leukocytes. FSC, forward scatter; SSC, side scatter.

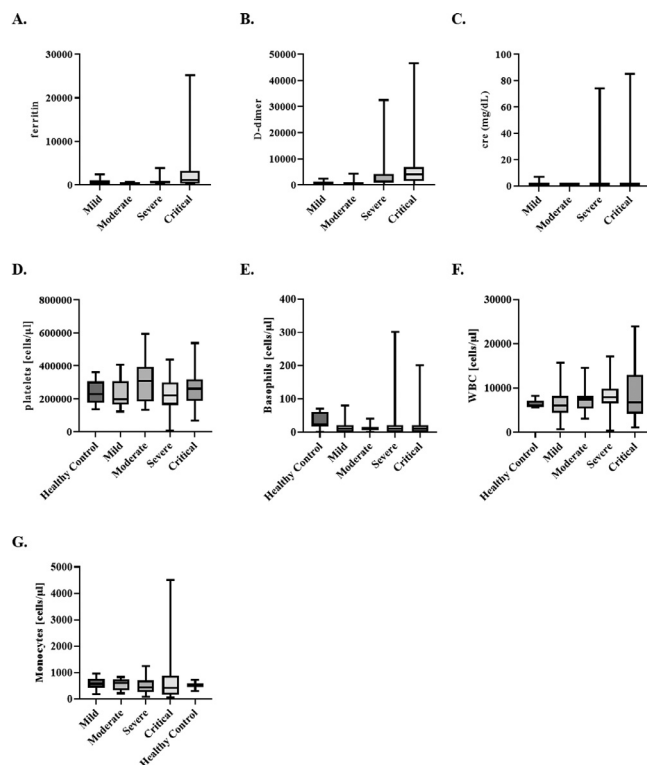


**Figure 2.** Laboratory findings of patients with COVID-19 and healthy controls: (A) Ferritin; (ng/mL) (B) d-Dimer; (ng/mL) (C) cre (mg/dL) levels; (D) platelets (cells/ $\mu$ L); (E) Basophils (cells/ $\mu$ L); (F) WBC (cells/ $\mu$ L); (G) Monocytes (cells/ $\mu$ L) from patients with COVID-19 and/or HCs. Data are shown as the mean  $\pm$  SEM. Asterisk denotes  $P < .05$ , double asterisks denote  $P < .01$ , triple asterisks denote  $P < .001$ , four asterisks denote  $P < .0001$ . COVID-19, coronavirus disease 2019; HCs, healthy controls; WBC, white blood cell.

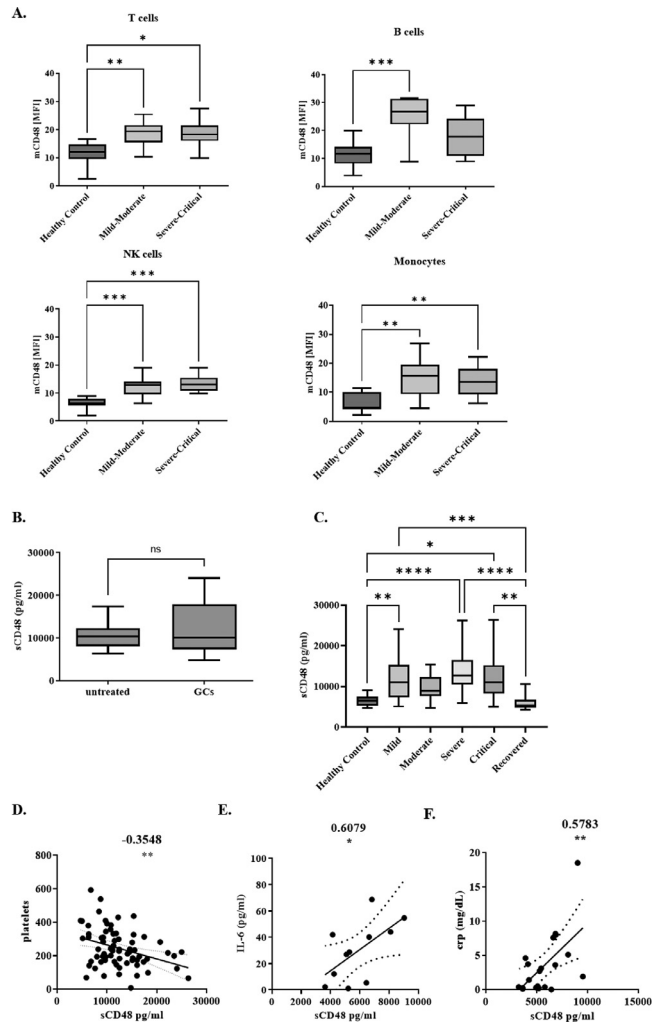


**Figure 3.** Membrane-associated and soluble CD48 levels of patients with COVID-19 and healthy controls: (A) mCD48 expression on peripheral blood leukocytes of patients with COVID-19 with different disease severity; (B) sCD48 levels in the sera of GCs of patients with treated or untreated COVID-19, (C) sCD48 levels in the sera of patients with different disease severity. Data are shown as the mean  $\pm$  SEM. Asterisk denotes  $P < .05$ , double asterisks denote  $P < .01$ , triple asterisks denote  $P < .001$ , four asterisks denote  $P < .0001$ . Pearson correlation analysis between sCD48 levels and (D) Platelets numbers; (E) IL-6; and (F) CRP levels of patients with COVID-19. COVID-19, coronavirus disease 2019; CRP, C-reactive protein; GCs, glucocorticosteroids; IL-6, interleukin-6; mCD48, membrane-bound CD48; sCD48, soluble CD48.